Visualizing Sphingosine-1-Phosphate Receptor 1($S1P_1$) Signaling During Central Nervous System De- and Re-Myelination

Ezzat Hashemi
Stanford University https://orcid.org/0000-0003-0868-4331
Hsing-Chuan Tsai
Kite Pharma Inc
Ezra Yoseph
Stanford University
Monica Moreno
Atara Biotherapeutic
Li-Hao Yeh
Chan Zuckerberg Biohub
Shalin B Mehta
Chan Zuckerberg Biohub
Mari Kono
NIDDK Genetics and Biochemistry Branch: National Institute of Diabetes and Digestive and Kidney Diseases Genetics and Biochemistry Branch
Richard Proia
NIDDK Genetics and Biochemistry Branch: National Institute of Diabetes and Digestive and Kidney Diseases Genetics and Biochemistry Branch
May Htwe Han (mayhan@stanford.edu)
Stanford University

Research Article

Keywords: Multiple sclerosis, demyelination, oligodendrocyte, sphingosine-1-phosphate receptor 1 and GFP reporter mice

Posted Date: June 30th, 2021

DOI: https://doi.org/10.21203/rs.3.rs-657784/v1

Abstract

Multiple sclerosis (MS) is an inflammatory demyelinating disease of the central nervous system (CNS) mediated by aberrant immune responses. The current immune modulatory therapies are unable to protect and repair the brain damage caused by the immune attack. One of the therapeutic targets for MS is the sphingosine-1-phosphate (S1P) pathways, which signals via sphingosine-1-phosphate receptors 1-5 ($S1P_{1-5}$), in the CNS and immune cells. In light of the potential neuro-protective properties of S1P signaling, we utilized the $S1P_1$-GFP (Green fluorescent protein) reporter mice in the cuprizone-induced-demyelination model, to investigate the *in vivo* S1P- $S1P_1$ signaling in the CNS. We observed $S1P_1$ signaling in a subset of neural stem cells in the subventricular zone (SVZ) during demyelination. Additionally, oligodendrocyte progenitor cells in the SVZ and mature oligodendrocytes in the medial corpus callosum (MCC) expressed $S1P_1$ signaling during remyelination. We did not observe $S1P_1$ signaling in neurons and astrocytes in the cuprizone model. This approach was unable to determine $S1P_1$-GFP signaling in the myeloid cells because of their aberrant GFP expression in GFP reporter mice. Significant $S1P_1$ signaling was observed in lymphocytes during demyelination and inflammation. Our findings reveal β-arrestin dependent $S1P_1$ signaling in oligodendrocyte lineage cells, indicating a role of $S1P_1$ signaling during remyelination.

Introduction

Multiple sclerosis (MS) is a chronic, progressive, inflammatory demyelinating disease of the

central nervous system (CNS) affecting more than two million young adults worldwide [1]. The pathological hallmarks of MS are CNS inflammation and dysregulated auto-reactive immune response [2]. Chronic neuroinflammation results in myelin loss, axonal damage and eventually neurodegeneration [3, 4]. Brain atrophy is observed in the very early stages of MS and secondary progression is associated with significant neurodegeneration [5, 6]. Current immune-modulatory therapies successfully suppress relapses but fail to halt progression and irreversible disability accumulation, indicating that mechanisms other than autoimmunity and aberrant immune response contribute to disease progression. Over time, approximately 80% of MS patients develop irreversible neurological disability and thereby become refractory to immunomodulatory therapies. Recognizing mechanisms dictating demyelination and repair in the CNS is essential to limit CNS injury, enhance repair and prevent permanent damage.

Sphingosine-1-phosphate (S1P) is a signaling molecule and has important regulatory functions in normal physiology and disease processes, particularly in cardiovascular, central nervous and immune systems. It can act as an intracellular mediator as well as a ligand for five specific high-affinity S1P receptor subtypes ($S1P_{1-5}$). S1P and its receptors ($S1P_{1-5}$) are crucial targets for immune regulatory functions such as lymphocyte development, egression, and adaptive immune response [7, 8]. S1P receptors are lipid G protein-coupled receptors (GPCRs) and express ubiquitously in all CNS cells [9, 10].

Previous reports reveal that, astrocytes express $S1P_{1,2,3,5}$, oligodendrocytes express $S1P_{1,3,5}$ and microglia express $S1P_{1,2,3,5}$ [10-12]. However, the mechanism of S1P signaling in the CNS remains unclear, due to receptor diversity, variation in expression levels, different signaling pathways and complex signaling functions. The recognition of S1P signaling in the CNS is important since multiple S1P receptor-specific modulators are in the pipeline for treatment of neurological disorders.

Clinical studies suggest that S1P receptor modulators directly affect the CNS beyond their immune modulatory function. For instance, Fingolimod (FTY720) is a $S1P_{1,3,4,5}$ modulator and a first-line immune modulatory therapy for relapsing-remitting MS [13]. Fingolimod enhances the production of various neuroprotective factors such as the brain-derived neurotrophic factor (BDNF) in microglia [14], while also increasing GABAergic transmission, cortical parvalbumin positive interneurons, axonal growth and regeneration [15-17]. FTY720 prevents dendritic spine loss and PSD-95 down-regulation in the hippocampus and attenuates Amyloid-b production in neurons [16, 18-20]. In MS, Fingolimod protects the brain from atrophy and halts disability progression; a feature lacking in most other therapies [20-22]. EXPAND studies indicate that Siponimod, a selective $S1P_{1,5}$ modulator, could reduce neurological injuries and progression of brain atrophy in secondary progressive MS [23, 24]. Increasing of S1P levels in cerebrospinal fluid, and a decrease of S1P in white matter and CNS lesions of MS patients further highlight the involvement of S1P signaling in neurodegeneration and inflammation [25, 26]. Taken together, these findings strongly suggest that S1P signaling is dysregulated in MS and that S1P targeting drugs may have direct beneficial effects on the CNS, independent of their immune modulatory function. However, whether S1P signaling has direct protective effects or whether it prevents inflammatory CNS damage via its immune modulatory function has not been clearly evaluated.

The present study aimed to investigate $S1P_1$ (S1P receptor 1) signaling during demyelination and repair in the CNS using GFP signaling mice, which are a potent model to reveal CNS signaling pathways. The cuprizone-induced demyelination model is a well-accepted model of CNS de- and re-myelination in the absence of overwhelming CNS inflammation caused by the peripheral immune response. In this study $S1P_1$-GFP signaling mice were exposed to a cuprizone diet for six weeks to induce demyelination followed by remyelination upon reintroduction of a regular diet. To analyze $S1P_1$-GFP signaling in the context of inflammatory demyelination, Experimental Autoimmune Encephalomyelitis (EAE) mice were utilized.

Our results revealed that upon cuprizone-induced demyelination a subtype of neural stem cells ($Sox2^+$ cells) in the SVZ express $S1P_1$ signaling. During remyelination, a subpopulation of oligodendrocyte progenitor cells ($NG2^+$ cells) and mature oligodendrocytes ($CC1^+$ cells) express $S1P_1$. No significant $S1P_1$ signaling was identified in neurons and astrocytes during de- or remyelination. In both the cuprizone and the EAE models a significant increase in lymphocyte (T and B cells) $S1P_1$ signaling was revealed by flow cytometry. In both models, myeloid cells showed aberrant GFP expression in GFP reporter mice. $S1P_1$-GFP signaling mice are an appropriate model to analyze $S1P_1$ signaling in

oligodendrocyte lineage cells during remyelination and lymphocytes in demyelination and inflammation phases.

Materials And Methods

Experimental Animals

The Tango design mice was used to monitor the $S1P_1$ signaling (S1P receptor 1) and signaling was visualized by the GFP reporter gene [27]. This model is able to detect $S1P_1$ signaling through β-arrestin interaction. In the Tango design mice, $S1P_1$ activation and coupling with β-arrestin released the tetracycline-controlled transactivator (tTA) from the C terminal of $S1P_1$, activating the histone-EGFP reporter gene (H2B-GFP) [27, 28]. The $S1P_1$ reporter mice were designed and developed by Kono, et al [27, 28]. Briefly, knock-in (ki) mice ($S1P_1$ki/ki) were generated with two fusion genes, with *S1Pr1* linked to tTA via a TEV protease cleavage site and mouse β-arrestin linked to TEV protease gene. The $S1P_1$ki/ki mice were crossed with a histone-EGFP reporter mouse (H2B-GFP; Tg(tetO-HIST1H2BJ/GFP)47Efu/J; The Jackson Laboratory), to derive the $S1P_1$-GFP signaling mice. The transgenic mice expressed the histone H2B-GFP controlled by a tetracycline-responsive element (TRE) upstream of a CMV promoter (**Figs. 1a, b**). GFP reporter mice with one allele of the H2B-GFP reporter gene was used as a control in our experiments. We used heterozygous knock-in allele ($S1P_1$ki/wt) mice with one allele of the H2B-GFP reporter gene to assay $S1P_1$ signaling in all of our experiments. These mice showed no phenotypic abnormalities. The mice were housed in groups of 3-5 within a 12-hour light/dark cycle at a controlled temperature with food and water provided *ad libitum*. All the animal protocols were approved by the Institutional Animal Care and Use Committee at Stanford University.

Polymerase Chain Reaction (PCR)

The $S1P_1$ knock-in genotypes were determined using PCR analyses of genomic DNA isolated from mouse tails. For genotyping by PCR, three primers were used, including 5'AGAGGAATGTGGGCTGTTGATCCT3' (primer one for knock-in), 5'AGATGGCGGTAACTCGAGG3' (primer two for the wild type), and 5'GGTTAGTGGTTGGCGATTAAATGCTGA3' (primer three as reverse). Primers one and three detected the $S1P_1$ knock-in allele and amplified a 612-bp fragment. Primers two and three detected the wild type allele and amplified a 405-bp fragment. In total, 40 cycles of 95°C (30 s), 62°C (30 s), and 72°C (45 s) were used for the amplification of these DNA segments. In addition, the GFP-reporter was detected by the two primers, $5TG\top\ CTGCTGGTAGTGGTCG3$ (reverse) and $5GCA\mathbb{C}ATC\top\ C\top\ C\forall\ GGACG3$ (forward) with a PCR product of 270 bp.

Cuprizone Experiments

The knock-in $S1P_1$-GFP signaling (H2B-GFP/$S1P_1$ki/wt) and H2B-GFP reporter (control) mice were fed with 0.2% cuprizone (TD.140800, ENVIGO) for six weeks followed by two weeks of normal chow. Brain

ntial time points during the cuprizone diet (weeks 0, 2, 4, and

6) and after two weeks of normal chow (week 8) (**Fig. 1c).** Male mice aged 3-4 months were used for all of the experiments (groups of 3-5).

Luxol Fast Blue (LFB) Stain

LFB was applied to brain sections to assess loss of myelin. Brain tissues were placed in 0.1% LFB at 60^{o}C overnight and then rinsed with 95% ethyl alcohol and distilled water. 0.05% lithium carbonate solution was used to differentiate the stained tissues for 10-30 seconds and further differentiation was performed with 70% ethyl alcohol for 10 seconds. Slides were counterstained with cresyl violet and dehydrated with 75%, 95% and 100% alcohol, cleared in xylene and then coversliped.

Quantitative Label-free Imaging

We used QLIPP, a quantitative label-free imaging method that measures the density and alignment of molecular assemblies using polarized light [29]. The method reports the alignment of molecular assemblies, such as myelin sheath, in terms of retardance. Retardance is the differential delay experienced by light polarized along the axis of the axon and perpendicular to the axon. More precisely, retardance is the difference in the optical path length experienced by light when it is polarized along two orthogonal orientations: along the symmetry axis of the molecular assembly and perpendicular to the symmetry axis of the assembly. Figure 3 demonstrates the use of optical anisotropy from QLIPP to study the amount of myelination in the white-matter region of the mouse brain without fluorescence label. [29].

Immunohistochemistry

Mice were anesthetized by inhalation of isoflurane and perfused with 25 ml phosphate buffered saline (PBS) into the left cardiac ventricle, followed by 25 ml of 4% paraformaldehyde (PFA) in PBS solution. Brains were post-fixed with 4% PFA for 12-16 hours and then transferred to 30% sucrose solution at 4^{o}C for 2-3 days until the tissue sank to the bottom of the container. Afterwards, the brains were embedded in a tissue freezing medium (Tissue-Tek O.C.T compound 4583, Sakura) and stored at -80°C. A cryostat-microtome (Leica CM 1850, Huston TX) was used for tissue sectioning (12 um) at -20 ^{o}C. Slides were stored at -20 or -80 ^{o}C until further use.

Immunofluorescence staining was performed to assess $S1P_1$ signaling in glial and neuronal cells during demyelination and repair using various antibodies, including MBP (AB7349, Abcam,1/300), CD68 (MCA1957GA, AbD Serotec, 1/300), Sox2 (AB5603, Millipore,1/250), Olig2 (MABN50, Millipore,1/400), NG2 (AB5320, Millipore,1/200), GFAP (20334, DAKO,1/700), NeuN (MAB377, Millipore,1/250), CC1 (OPBO, calbiochem,1/300) and EDG1 (ab23695 Abcam,1/150). To complete immunofluorescence, slides were preserved at 37 ^{o}C for 15-30 minutes and washed twice in PBST (PBS+Tween-20 [0.1%]) for five minutes each time. Sodium citrate buffer (10Mm, PH=6) and heat-induced antigen retrieval method were utilized for Olig2 and CC1 staining. Nonspecific signaling was blocked using 5% serum (normal goat serum [G9023, Sigma]) and the sections were incubated using antibodies diluted in PBS-Triton-100X 0.1% + 1%

 Secondary antibodies, anti-rat Alexa Flour 555 (A21434,

Invitrogen, 1/1000), anti-rabbit Alexa Flour 555 (A21428, Invitrogen, 1/1000), anti-mouse Alexa Flour 555 (A21424, Invitrogen, 1/1000), anti-mouse Alexa Flour 647 (A32728, Invitrogen, 1/1000) and anti-rabbit Alexa Flour 647 (A27040, Invitrogen, 1/1000) were used for labeling. The slides were then counterstained with DAPI and coverslipped. A Keyence microscope (BZ-X700 series) was used to evaluate staining and take pictures. ImageJ software was applied for cell counting and intensity measurements. Blind count and manual counting performed by ImageJ with higher magnification.

EAE Experiments

EAE was induced in male $S1P_1$ -GFP signaling mice and GFP reporter mice aged 8-12

weeks. According to methods defined by Tsai et al [30, 31], mice were immunized with an emulsion containing 200 micrograms of Complete Freund's Adjuvant (CFA), 100 micrograms of myelin oligodendrocyte glycoprotein (MOG_{35-55}) peptide35–55, and 200 nanograms of *Bordetella pertussis* toxin (lot# 181236A1, List Biological Laboratories) on days zero and two. The spleen tissues were collected after eight days of immunization which marked the onset of the clinical EAE symptoms.

GFP Signaling in the Immune Cells Isolated from Brain and Spleen Using Flow Cytometry

Brain and spleen of cuprizone-fed mice were collected at weeks 0, 2, 4, and 6 to analyze $S1P_1$ signaling in immune cells. In order to evaluate $S1P_1$ signaling in the inflammatory state, $S1P_1$ signaling was also examined in the spleen of EAE mice. Immune cells obtained from brain and spleen were isolated as previously reported [32]. Briefly, mice were anesthetized and then perfused with 25 ml cold PBS. The spleens were removed before perfusion and homogenized through a 70-μm cell strainer. Red blood cells (RBC) were lysed by ACK lysing buffer (0.15 M NH_4Cl, 10 mM $KHCO_3$, and 0.1 M $EDTANa_2.H_2O$ 3.7) for 30-60 seconds and then washed with PBS; 10^6 cells were used for labeling with antibody. Brains were collected after PBS perfusion and homogenized through a 70-μm cell strainer in sterile PBS and then centrifuged. The pellet was treated with collagenase II (1mg/ml) for 1 hour at 37 °C. The collagenase reaction was stopped by adding PBS to the cells and centrifugation. Immune cells were harvested from a 30% Percoll gradient by centrifugation, and residual red blood cells were lysed by ACK lysing buffer for 5-10 seconds. The immune cells were washed with PBS and 0.5–1 × 106 cells were labeled with individual antibodies and analyzed using the LSRII Flow Cytometer (BD) at the Stanford core Facility. BD FACS Diva 6.0 software was used to acquire data and FlowJo was employed for data analysis (Tree Star). The monoclonal antibodies used in flow cytometry analysis were purchased from the following sources: anti-CD45 (clone 30-F11), anti-CD3 (clone 145-2c11), anti CD4 (clone GK1.5), anti CD8 (clone 53–6.7), anti CD19 (clone 6D5), anti-CD11b (clone M1/70), anti-CD11c (clone N418), anti-Ly6C (clone HK1.4), and anti-Ly6G (clone 1A8). Single color-stained BD-CompBeads (BD Bioscience) were used to set compensation and gating the stained cells. CNS immune cells were gated by multi-dimensional flow cytometry. First, cells were gated into $CD45^{lo}$ and $CD45^{hi}$ from live leukocytes. $CD45^{lo}$ cells represent microglia and $CD45^{hi}$ represent infiltrating immune cells (**Supplementary Fig. 1S**). $CD45^{hi}$ cells were gated to CNS-infiltrating

ytes ($CD45^{hi}CD3^+$). Infiltrating myeloid cells ($CD45^{hi}CD11b^+$)

were further gated to monocyte derived dendritic cells ($CD45^{hi}CD11b^{+}Cd11c^{+}$) and myeloid cells ($CD45^{hi}CD11b^{+}CD11c^{-}$). Afterwards $CD11b^{+}CD11c^{-}$ myeloid cells were separated into neutrophils ($Ly6C^{-}Ly6G^{+}$) and monocytes ($Ly6C^{+}Ly6G^{-}$). GFP expression was assessed in brain myeloid cells ($CD45^{hi}CD11b^{+}$), granulocytes ($CD11b^{+}Ly6C^{-}Ly6G^{+}$) and lymphocytes ($CD45^{hi}CD3^{+}$). Splenic cells were gated as myeloid cells ($CD45^{+}CD11b^{+}$) and lymphocytes ($CD45^{+}CD3^{+}$), GFP expression was assessed in splenic myeloid cells and lymphocytes. In EAE mice, splenic cells were collected as outline above and were gated as myeloid cells ($CD45^{+}CD11b^{+}$), T cells ($CD45^{+}CD3^{+}$) and B cells ($CD45^{+}CD19^{+}$).

Statistical Analyses

Data analysis was performed in GraphPad Prism 8 and results are expressed as mean standard error of the mean (SEM). Unpaired t-test was applied for the statistical analysis of the two study groups, and statistical significance was determined by calculating the *P*-value (**P*<0.05, ***P*<0.01, ****P*<0.001 and *****P*<0.0001).

Results

Validation of Cuprizone-Induced Demyelination in S1P1-GFP Signaling Mice

Cuprizone causes immediate damage to the oligodendrocytes which consequently leads to demyelination [33]. To validate demyelination in the S1P1-GFP signaling mice following exposure to cuprizone diet, myelin basic protein (MBP) intensity was measured in the medial corpus callosum (MCC) and oligodendrocytes in the MCC were counted. ImageJ was used for cell counting and measuring of MBP intensity. The results indicated a significant decrease in MBP intensity in the medial corpus callosum after 4 weeks of cuprizone diet, ***p<0.001 (Figs. 2a, C). LFB test was carried out, indicating a reduction in myelin after 4 weeks of cuprizone diet (Fig. 2b). In addition, we used a quantitative label-free imaging method, QLIPP, to measure the optical anisotropy (retardance), which arises from ordered molecular structures such as myelin, for visualizing the distribution of myelin in MCC without a label [29]. Label free imaging of myelination indicates a significant difference in retardance (myelination level) in MCC after 4 weeks of cuprizone diet (Fig. 3).

Oligodendrocyte number decreased at 2 weeks of cuprizone diet and returned to normal at 4 weeks, *p<0.05 (Supplementary, Fig. 2S-a, d). Another important pathological feature of cuprizone-induced demyelination was astrocytosis, the peak of which was observed after 4 weeks of cuprizone diet (Supplementary, Fig. 2S-b). Active myeloid cells (CD68+ cells) were observed in the corpus callosum (CC), hippocampus, amygdala, caudoputamen and septofimberial nucleus at 2 weeks of cuprizone diet (Supplementary, Fig. 2S-c). Furthermore, CD68+ cell number increased in the CC, hippocampus, primary somatosensory cortex, caudoputamen and preoptic area at 4 weeks of cuprizone diet. After 6 weeks of cuprizone diet, CD68+ cells were present in the CC, hippocampus, amygdala, and thalamus. At 8 week (remyelination), CD68+ cells were still observed in the CC, deep layer of the cortex, thalamus, and dorsal

hippocampal commissure. In total, myelin loss, astrocytosis, reduced oligodendrocyte number, and increased CD68+ cells confirmed the effects of cuprizone on S1P1-GFP signaling mice.

GFP Signaling in the CNS During Cuprizone-induced de- and re-myelination

Based on the Tango design, S1P1 signaling is visualized by GFP expression. S1P1-GFP signaling was analyzed in CNS glia and neurons during demyelination following exposure to cuprizone diet (weeks 0-6) and upon remyelination (normal diet weeks 6-8) (Fig. 1c). The number of GFP+ cells increased during the cuprizone diet in the CC. After 2 weeks, GFP+ cells appeared in the brain and reached a maximum at week 4. The cells in lateral corpus callosum (LCC) and MCC of the S1P1-GFP signaling mice displayed the highest expression of GFP (Supplementary, Fig. 3S-a, c). GFP signaling was also detected in the CC of the GFP reporter mice at various time points of the cuprizone diet (Supplementary, Fig. 3S-b, d). GFP reporter mice showed less GFP+ cells in the CC than GFP-S1P1 signaling mice at 2, 4, and 6 weeks of the cuprizone diet but the difference was not statistically significant (Supplementary, Fig. 3S-e).

GFP Signaling in the CNS cells during demyelination and repair

We then investigated S1P1 signaling in neurons and CNS glia of S1P1-GFP signaling mice during cuprizone-induced de- and -remyelination. GFP expression was assessed in oligodendrocytes, neurons, neuronal stem cells, astrocytes and CNS myeloid lineage cells.

S1P1-GFP Signaling in Oligodendrocytes During Remyelination

S1P1 plays a key role in oligodendrocyte morphology and differentiation [34-37]. We quantified the number of Olig2+ cells in the MCC of cuprizone-fed S1P1-GFP signaling mice by immunohistochemistry. The MCC of S1P1-GFP signaling mice showed a decreased number of oligodendrocytes (n=3, *P<0.05) at two weeks of cuprizone diet (Supplementary, Fig. 2S-a, d). 2.3 ± 0.3% of the GFP+ cells in the MCC of S1P1-GFP signaling mice were positive for Olig2 after 4 weeks of cuprizone diet (Fig. 4a, e). After 6 and 8 weeks of cuprizone diet, 11± 0.5% and 9.8 ± 0.8% of the GFP+ cells were Olig2+ respectively (Fig. 4b, c, e). To verify the specificity of GFP signaling, S1P1 staining was performed and most of GFP+Olig2+ cells were positive for S1P1 (Fig. 4d). Compared with S1P1-GFP signaling mice, only 2.3% and 3.3% of GFP+ cells of GFP reporter mice expressed Olig2+ in the corpus callosum at weeks 6 and 8 of the cuprizone diet respectively (Fig. 4e). Olig2+ cells in CC express higher GFP in S1P1-GFP signaling mice compared to GFP reporter mice. Sox2, a critical transcription factor in neural stem cells, is essential for oligodendrocyte progenitor cell (OPC) proliferation and oligodendrocyte regeneration following myelin impairment in the adult brain [38]. Oligodendrocytes express NG2 in early stage of their development. However, NG2+ cells are able to differentiate to gray matter astrocyte and pericytes [39-41]. Sox2 and NG2 staining was performed along with quantification of cells with GFP expression. S1P1 signaling was distinguished in 5% of Sox2+ cells in the SVZ of cuprizone-fed mice during demyelination (4 weeks) (Fig. 5a). The number of the Sox2+ cells decreased in the SVZ at 2-4 weeks of cuprizone diet, but the change was not statistically significant (Fig. 5d). 10.33 ± 2.6% and 9 ± 2% of the GFP+ cells were Sox2+ in 4 and

6 weeks cuprizone fed respectively but Sox2+ cells did not express significant S1P1 signaling during remyelination (Fig. 5e).

Approximately 70% of the NG2+ cells in the SVZ of S1P1-GFP signaling mice were Olig2+ cells during remyelination (Supplementary, Fig. 4S). Oligodendrocyte precursor cells (NG2+Olig2+) express GFP during remyelination (Fig. 5b). NG2+ cells in the SVZ increased significantly at 2 weeks, *p<0.05. An increase of NG2+ cells during remyelination (8 weeks) did not reach statistical significance (Fig. 5f). NG2+ cells were negative for S1P1 signaling at 2 weeks of cuprizone diet, whereas around 2% of GFP+ cells were NG2+ in the SVZ at 8 weeks (Fig. 5g). Sox2+ cells expressed GFP during demyelination but NG2+ cells expressed GFP during remyelination.

In order to analyze GFP expression in mature oligodendrocytes, CC1 (a marker for mature oligodendrocytes) staining was performed, showing that 10.5 ± 2.4% of the GFP+ cells were CC1-positive after 8 weeks of cuprizone diet (Fig. 5c, h). In conclusion, S1P1 signaling is observed in immature progenitor oligodendrocytes (NG2+ cells) in the SVZ and in mature oligodendrocytes (CC1+ cells) in the MCC during remyelination. The Olig2+GFP+ cells may represent S1P1 signaling through β-arrestin in oligodendrocytes.

No Significant S1P1 Expression in Astrocytes During De- and Re-myelination

FTY720 is a S1P1-3-4-5 modulator, which downregulates NF-κB signaling in astrocytes, thereby decreasing the expression of proinflammatory and neurotoxic mediators [42]. Moreover, SEW2871, a selective S1P1 agonist, stimulates astrocyte migration [43]. In order to determine whether GFP expression is correlated with S1P1 signaling in astrocytes, GFAP staining was assessed. GFAP+ cells did not express GFP signaling during de- and re-myelination (weeks 2, 4, 6 and 8) (Fig. 6a).

S1P1 Signaling Is not Detected in Mature Neurons

Previous reports indicated that the S1P1-3-4-5 modulator, FTY720, suppressed neuronal injury and improved cognition after cerebral ischemia [44]. In the present study, the role of neuronal S1P1 signaling was further investigated during demyelination and repair. An immunofluorescence test with NeuN staining was performed but S1P1 signaling was not detected in the neurons of the CC, hippocampus and cortex (Fig. 6b).

Myeloid Cell-S1P1 Signaling in S1P1-GFP Signaling Mice During De- and Re-myelination

Our previous research indicated that myeloid S1P1 signaling plays a key role in CNS autoimmunity and neuroinflammation [31]. Previous reports suggest that S1P1 regulates pro and anti-inflammatory microglia (M1/M2) polarization, and a study by Gaire (2019) demonstrated that the suppression of S1P1 activity attenuates M1 polarization and induces the M2 phenotype [45]. Considering the key role of S1P1 in microglia polarization, we investigated S1P1 signaling in CNS myeloid-lineage cells, infiltrating monocytes and microglia. CD68 immunofluorescence staining was performed on brain sections of

s (weeks 0, 2, 4, 6 and 8). At two weeks of cuprizone diet,

almost 92% of GFP+ cells in CC were positive for CD68, whereas at weeks 4, 6, and 8 only 80-76-83% of GFP+ cells also expressed CD68+ in CC respectively (Fig. 7a, Supplementary Fig. 5S). Unexpectedly, GFP expression was also observed in CD68+ cells of GFP reporter mice at 4, 6 and 8 weeks of cuprizone diet (Fig. 7b). The colocalization of GFP and CD68 in GFP reporter and S1P1-GFP signaling mice indicates that GFP signaling is not associated with S1P1 signaling. Naïve GFP reporter and S1P1-GFP signaling mice did not express GFP, however, following exposure to cuprizone diet myeloid cells in both groups expressed GFP signaling.

To validate the outcomes of the study, myeloid cells and lymphocytes were examined in the brain and spleen of mice with cuprizone-induced demyelination using flow cytometry.

Gating strategy for CNS immune cells is shown in supplementary Fig. 1S. The number of CNS infiltrating myeloid cells (CD45hiCD11b+), lymphocytes (CD45hiCD3+) and granulocytes (CD45hi CD11b+Ly6G+) increased significantly at 2-week of cuprizone diet (**p<0.01, *p<0.05 and **p<0.01 respectively) in S1P1-GFP signaling mice. However, both GFP reporter and S1P1-GFP signaling mice expressed GFP in myeloid cells and granulocytes. Lymphocytes (CD3+) showed higher but not statistically significant GFP signaling in the brain of S1P1-GFP signaling mice compared to the GFP reporter mice after 2 and 4 weeks of cuprizone diet (Fig. 8c, g and supplementary Fig. 6S-c, g). The expression of GFP in microglia (CD45lo CD11b+) increased significantly in GFP reporter and S1P1-GFP signaling at 4 weeks cuprizone-fed (*p<0.05) (Fig. 8i, j and supplementary Fig. 6S-i, j).

It could not be confirmed whether GFP leakiness was limited to CNS myeloid cells. Therefore, splenic myeloid cells and lymphocytes were assessed in GFP-reporter and S1P1-GFP signaling cuprizone-fed mice. Myeloid cells (CD45+CD11b+) decreased significantly in the spleen after 2 weeks of cuprizone diet (*P<0.05). However, no significant difference was observed in the GFP+CD11b+ cells between GFP reporter and S1P1-GFP signaling mice. The CD3+ cells increased significantly in the spleen after 2 and 4 weeks of cuprizone diet (*p<0.05). Interestingly, GFP+CD3+ cells were significantly more abundant in S1P1-GFP signaling mice compared to the GFP reporter mice after 2 and 6 weeks of cuprizone diet (**p<0.01 and *p<0.05, respectively) (Fig. 9 and supplementary Fig. 7S).

Confirmation of S1P1 Expression in Immune Cells in the EAE Model

Myeloid S1P1 signaling was investigated in EAE mice, an animal model of MS. Flow cytometry was performed to characterize S1P1 signaling in myeloid cells and lymphocytes during inflammation. While splenic myeloid cells (CD45+CD11b+) expressed high levels of GFP in both the EAE GFP reporter and S1P1-GFP signaling mice (Supplementary Fig. 8S), GFP expression was significantly higher in splenic lymphocytes of S1P1-GFP signaling mice. Splenic B (CD19+) and T cells (CD3+) of EAE mice expressed significantly higher GFP signaling compared to the control group during inflammation (Supplementary Fig. 9).

Discussion

$S1PR_{1-5}$ modulators, such as Fingolimod and Siponimod, reduce neurological injuries and progression of brain atrophy in secondary progressive MS, but mechanisms underlying S1P signaling in the CNS cells entail further studies. The complexity of $S1PR_{1-5}$ signaling assessment results from ubiquitous expression in various cell types and the promotion of different signaling pathways through association with different G proteins which employs various cell behaviors. Nevertheless, expression levels, function and mechanism of each receptor subtype in neurons and glial cells during demyelination, neurodegeneration and repair remain elusive. In this study, we used $S1P_1$-GFP signaling mice to analyze, $S1P_1$ signaling in the CNS during de- and re-myelination using a cuprizone model. To the best of our knowledge, this is the first study to analyze $S1P_1$ signaling *in vivo* via GFP expression in CNS cells during de- and re-myelination.

One of the objectives of the current research was to determine whether oligodendrocytes express $S1P_1$ signaling during toxic insult and repair. According to the literature, S1P receptors are expressed in the oligodendrocyte lineage. For instance, FTY720 regulates the survival and maturation of OPCs [34, 35]. $S1P_1$ conditional knockout mice displayed a reduction in myelin thickness in the CC and $S1P_1$-deficient oligodendrocytes had slower process extension [37]. However, previous studies indicated that cuprizone feeding does not increase cell death in $S1P_1$-deficient oligodendrocytes [46]. $S1P_1$ signaling is essential for neural stem cell mobilization and migration to sites of CNS injury and also plays a major role in oligodendrocytes differentiation [47-49]. Also, Sox2 is crucial for oligodendrocyte proliferation and differentiation in the adult brain [48]. $S1P_1$ signaling in neural stem cells ($Sox2^+$ cells) during demyelination suggest a role in proliferation and differentiation of neural stem cells to oligodendrocytes and/or migration of neural stem cells to the site of injury. Our results showed $S1P_1$ signaling in immature and mature oligodendrocytes during remyelination (**Figs. 5e, g, h**) which implicate $S1P_1$ signaling in differentiation, maturation, survival and morphology of oligodendrocytes. Heterogeneity in oligodendrocyte lineage cells and dynamics of oligodendrocyte differentiation and maturation [50, 51] may be the reason for β-arrestin dependent $S1P_1$ signaling in subpopulation of oligodendrocytes. In support of our findings related to MS, other studies have reported a decrease of S1P in the white matter and CNS lesions of MS patients. Further, it is known that fingolimod prevents brain atrophy and halts disability progression, and Siponimod reduces neurological injuries and progression of brain atrophy in secondary progressive MS.

Previous studies reported protective effects of $S1P_1$ signaling in neurons after ischemic stroke [52] . Furthermore, $S1P_1$ signaling regulates glutamate secretion and synaptic transmission [53]. However, in the present study, β-arrestin dependent $S1P_1$ signaling was not detected in neurons during de- and -remyelination. $S1P_1$ signaling is essential for switching the intermediate/transition astrocytes to reactive astrocytes [54]. Hypertrophic astrocytes in the brain lesions of MS patients express $S1P_1$ [55, 56]. The high arborization and density of astrocytes during demyelination made it difficult to determine the exact number of the GFP^+GFAP^+ cells by immunofluorescence. To overcome this difficulty in our analyses, we as located in the cell body of the astrocytes rather than

around the arborization. Nevertheless, $S1P_1$ signaling was not distinguished significantly in astrocytes of $S1P_1$-GFP signaling mice. The absence of $S1P_1$ signaling in neurons and astrocytes can be interpreted by low levels of $S1P_1$ expression and/or reduced turnover of these cells. Also, β-arrestin independent signaling and involvement of other S1P receptor subtypes (such as $S1P_3$) may account for the lack of $S1P_1$ signaling in neurons and astrocytes reported here [57].

$S1P_1$ is the major S1P receptor expressed in immune cells and plays a pivotal role in immune cell function, development and trafficking. Lymphocyte exit from secondary lymphatic organs into the systemic circulation is regulated by $S1P_1$ signaling [8, 58]. Moreover, $S1P_1$ is essential for the transfer of immature B cells from the bone marrow to the circulation[59].

In the current research, lymphocytes and myeloid cells were examined in the brain and spleen of mice with cuprizone-induced demyelination by flow cytometry. Remarkably, splenic lymphocytes ($CD3^+$) expressed significantly higher levels of GFP in $S1P_1$-GFP signaling mice compared to the GFP reporter mice. Another objective of the present study was to determine whether GFP expression was specific in lymphocytes during inflammation. To this end, EAE mice were used as an animal model of MS, and specific GFP signaling was observed in splenic T cells and B cells ($CD3^+$ and $CD19^+$) during inflammation in the EAE GFP-$S1P_1$ signaling mice compared to GFP reporter mice. The subpopulations of T cells, $CD8^+$ and $CD4^+$ cells, expressed significantly higher $S1P_1$ signaling in EAE GFP-$S1P_1$ signaling mice compared to GFP reporter mice. These results demonstrated that increased $S1P_1$ signaling in splenic lymphocytes during demyelination and inflammation occurs in a β-arrestin dependent manner. Previous studies have shown increased S1P concentration in the CSF of MS subjects. Higher levels of S1P in the CSF may provoke immune cells trafficking in the CNS and inhibit T(reg) function via β-arrestin dependent $S1P_1$ signaling [60, 61].

Several preclinical studies have demonstrated the effects of S1P signaling on microglia. For example, FTY720 upregulates the brain-derived neurotrophic factor and downregulates production of pro-inflammatory cytokines in microglia [14] . In myeloid cells $S1P_1$ signaling is critical in the polarization of M1/M2 macrophages [62]. Our previous research demonstrated that continuous $S1P_1$ signaling in myeloid cells mediates T_H17 polarization [31]. GFP expression in GFP reporter mice should be silent in the absence of tTA. However, our immunohistochemistry and flow cytometry tests indicated aberrant expression of the transgene in activated myeloid cells in the GFP reporter mice after EAE and cuprizone induced demyelination. Previous studies have identified GFP leakage in hematopoietic stem cells in H2B-GFP reporter mice [63, 64]. Putative GFP leakage prevents us from drawing any conclusions regarding $S1P_1$-GFP signaling in CNS resident and peripheral myeloid cells. Several studies have reported accuracy and reliability of the $S1P_1$-GFP signaling murine model [27, 65]. However, none of these studies investigated CNS inflammations and activated myeloid cells. The causes of the aberrant GFP expression in the absence of the tTA protein remain unclear. It is possible that the H2B-GFP transgene was integrated into a region of DNA in the myeloid cells, switching the transcriptional activity by the cuprizone diet or

EAE induction. H2B-GFP protein in the nucleosome may affect the chromatin structure and gene expression in the activated myeloid cells, as well as our findings regarding the potential leakiness of GFP. Non-specific binding to the synthetic promoter in activated microglia may be another cause of the GFP leakiness. S1P could also act as an intracellular messenger and bind to nuclear $S1P_1$, which inhibits the activity of histone deacetylase 1 and 2 (HDAC1/2), thereby resulting in epigenetic regulation of gene expression [66, 67]. Modulation of HDAC1/2 by nuclear $S1P_1$ may also account for the GFP leakiness in myeloid cells.

β-arrestins act as multifunctional adaptors for activated GPCRs including $S1P_1$. β-arrestin-dependent signaling is extremely diverse and incites distinct cellular responses. The binding of β-arrestin to the intracellular domain can halt G protein-mediated signaling and desensitize $S1P_1$ signaling. The association of β-arrestin with $S1P_1$ can initiate endocytic machinery and internalize the $S1P_1$. Activated β-arrestin supports multiple components of a kinase cascade and propagating specific signaling pathway [68, 69]. Consequently, $S1P_1$- β-arrestin signaling can create different cell behaviors in CNS glial cells and immune cells.

In summary, our results indicate that the $S1P_1$ signaling in the oligodendrocyte lineage during remyelination may have a protective effect by regulating myelination in response to injury. Elucidating regulatory mechanisms downstream of $S1P_1$- β-arrestin signaling in oligodendrocytes will provide important evidence to design effective therapies for demyelinating diseases like MS. $S1P_1$ was not significantly expressed in neurons and astrocytes, possibly because $S1P_1$ signaling in CNS neurons and astrocytes is not dependent on β-arrestin.

$S1P_1$ signaling was identified in lymphocytes during demyelination and inflammation. In this regards, $S1P_1$-GFP signaling mice could be used to analyze the anti-inflammatory role of $CD3^+$ cells, as well as the role of B cells in neurodegeneration and repair in EAE and cuprizone models.

Flow cytometry and immunofluorescence detected GFP leakage upon EAE induction and cuprizone exposure in GFP reporter mice, complicating interpretation. It is essential to generate new lines of H2B-GFP reporter mice to demonstrate appropriate reporter for analysis of myeloid cells.

Abbreviations

CC: Corpus Callosum

CNS: Central Nervous System

CP: Caudo-Putamen

CTX: Cortex

yelitis

GFAP: Glial Fibrillary Acidic Protein

GFP: Green Fluorescence Protein

GPCR: G protein-coupled receptor

HDAC1/2: Histone Deacetylase 1 and 2

IRES: Internal Ribosome Entry Site

LCC: Lateral Corpus Callosum,

LFB: Luxol Fast Blue

MBP: Myelin Basic Protein

MCC: Medial Corpus Callosum

MS: Multiple sclerosis

NG2: Neural/Glial Antigen

OPCs: Oligodendrocyte Progenitor Cells

QLIPP: *quantitative label-free imaging* with phase and polarization

S1P: Sphingosine-1-phosphate

S1pr1: S1P receptor 1 gene

$S1P_1$: S1P receptor 1

$S1PR_{1\text{-}5}$: Sphingosine-1-phosphate receptors 1-5

SVZ: Subventricular Zone

TEV: Tobacco Etch Virus

Declarations

Data Availability

Please contact the authors for data requests.

Funding

This study was supported by Fondation Leducq and a training grant from National Institutes of Health on infection, Immunity, and Inflammation (T32 AI 7290-32).

Contributions

Ezzat Hashemi (E.H.): designed and performed the experiments, analyzed and interpreted the data, made figures and wrote the manuscript. Hsing-Chuan Tsai (T.S.) performed EAE experiments and helped in flowcytometry tests and analysis. Ezra Yoseph (E.Y.) performed IHC tests and cell counting. Monica Moreno (M.M.) collaborated in tissue collection and data acquisition. Li-Hao Yah (L.Y.) and Shalin B Mehta (S.M.) analyzed myelin by label-free imaging. Mari Kono (M.K.) and Richard Proia (R.P.) provided $S1P_1$-GFP signaling mice and contributed to the final manuscript. May H Han (M.H.) designed the experiments, analyzed, and interpreted the data and supervised the study. All authors read and approved the final manuscript.

Acknowledgements

We thank our collogues Nora Sandrine Wetzel and Anna Tomczak for manuscript critical review.

Competing Interests

The authors declare that they have no conflicts of interest.

Ethic Approval and Consent to Participant

All methods and animal procedures were performed in accordance with The Guide for the Care and Use of Laboratory Animals and were reviewed and approved by the Institutional Animal Care and Use Committee at Stanford University.

Consent to Participant

Not applicable

Consent for Publication

Not applicable

Code availability

Not applicable

References

1. Collaborators GBDMS: Global, regional, and national burden of multiple sclerosis 1990-2016: a systematic analysis for the Global Burden of Disease Study 2016. *Lancet Neurol* 2019, 18(3):269-285.

2. Baecher-Allan C, Kaskow BJ, Weiner HL: Multiple Sclerosis: Mechanisms and Immunotherapy. *Neuron* 2018, 97(4):742-768.

3. Rotshenker S: Wallerian degeneration: the innate-immune response to traumatic nerve injury. *J Neuroinflammation* 2011, 8:109.

4. Conforti L, Gilley J, Coleman MP: Wallerian degeneration: an emerging axon death pathway linking injury and disease. *Nat Rev Neurosci* 2014, 15(6):394-409.

5. Andravizou A, Dardiotis E, Artemiadis A, Sokratous M, Siokas V, Tsouris Z, Aloizou AM, Nikolaidis I, Bakirtzis C, Tsivgoulis G *et al*: Brain atrophy in multiple sclerosis: mechanisms, clinical relevance and treatment options. *Auto Immun Highlights* 2019, 10(1):7.

6. Popescu V, Agosta F, Hulst HE, Sluimer IC, Knol DL, Sormani MP, Enzinger C, Ropele S, Alonso J, Sastre-Garriga J *et al*: Brain atrophy and lesion load predict long term disability in multiple sclerosis. *J Neurol Neurosurg Psychiatry* 2013, 84(10):1082-1091.

7. Blaho VA, Hla T: An update on the biology of sphingosine 1-phosphate receptors. *J Lipid Res* 2014, 55(8):1596-1608.

8. Cyster JG, Schwab SR: Sphingosine-1-phosphate and lymphocyte egress from lymphoid organs. *Annu Rev Immunol* 2012, 30:69-94.

9. Nishimura H, Akiyama T, Irei I, Hamazaki S, Sadahira Y: Cellular localization of sphingosine-1-phosphate receptor 1 expression in the human central nervous system. *J Histochem Cytochem* 2010, 58(9):847-856.

10. Groves A, Kihara Y, Chun J: Fingolimod: direct CNS effects of sphingosine 1-phosphate (S1P) receptor modulation and implications in multiple sclerosis therapy. *J Neurol Sci* 2013, 328(1-2):9-18.

11. Soliven B, Miron V, Chun J: The neurobiology of sphingosine 1-phosphate signaling and sphingosine 1-phosphate receptor modulators. *Neurology* 2011, 76(8 Suppl 3):S9-14.

12. O'Sullivan S, Dev KK: Sphingosine-1-phosphate receptor therapies: Advances in clinical trials for CNS-related diseases. *Neuropharmacology* 2017, 113(Pt B):597-607.

13. Khatri BO: Fingolimod in the treatment of relapsing-remitting multiple sclerosis: long-term experience and an update on the clinical evidence. *Ther Adv Neurol Disord* 2016, 9(2):130-147.

14. Noda H, Takeuchi H, Mizuno T, Suzumura A: Fingolimod phosphate promotes the neuroprotective effects of microglia. *J Neuroimmunol* 2013, 256(1-2):13-18.

15. Gentile A, Musella A, Bullitta S, Fresegna D, De Vito F, Fantozzi R, Piras E, Gargano F, Borsellino G, Battistini L *et al*: Siponimod (BAF312) prevents synaptic neurodegeneration in experimental multiple

sclerosis. *J Neuroinflammation* 2016, 13(1):207.

16. Anastasiadou S, Knoll B: The multiple sclerosis drug fingolimod (FTY720) stimulates neuronal gene expression, axonal growth and regeneration. *Exp Neurol* 2016, 279:243-260.

17. Szepanowski F, Derksen A, Steiner I, Meyer Zu Horste G, Daldrup T, Hartung HP, Kieseier BC: Fingolimod promotes peripheral nerve regeneration via modulation of lysophospholipid signaling. *J Neuroinflammation* 2016, 13(1):143.

18. Fukumoto K, Mizoguchi H, Takeuchi H, Horiuchi H, Kawanokuchi J, Jin S, Mizuno T, Suzumura A: Fingolimod increases brain-derived neurotrophic factor levels and ameliorates amyloid beta-induced memory impairment. *Behav Brain Res* 2014, 268:88-93.

19. Doi Y, Takeuchi H, Horiuchi H, Hanyu T, Kawanokuchi J, Jin S, Parajuli B, Sonobe Y, Mizuno T, Suzumura A: Fingolimod phosphate attenuates oligomeric amyloid beta-induced neurotoxicity via increased brain-derived neurotrophic factor expression in neurons. *PLoS One* 2013, 8(4):e61988.

20. Zhang J, Xiao B, Li CX, Wang Y: Fingolimod (FTY720) improves postoperative cognitive dysfunction in mice subjected to D-galactose-induced aging. *Neural Regen Res* 2020, 15(7):1308-1315.

21. Smith PA, Schmid C, Zurbruegg S, Jivkov M, Doelemeyer A, Theil D, Dubost V, Beckmann N: Fingolimod inhibits brain atrophy and promotes brain-derived neurotrophic factor in an animal model of multiple sclerosis. *J Neuroimmunol* 2018, 318:103-113.

22. De Stefano N, Silva DG, Barnett MH: Effect of Fingolimod on Brain Volume Loss in Patients with Multiple Sclerosis. *CNS Drugs* 2017, 31(4):289-305.

23. Benedict RHB, Tomic D, Cree BA, Fox R, Giovannoni G, Bar-Or A, Gold R, Vermersch P, Pohlmann H, Wright I *et al*: Siponimod and Cognition in Secondary Progressive Multiple Sclerosis: EXPAND Secondary Analyses. *Neurology* 2021, 96(3):e376-e386.

24. Leavitt VM, Rocca M: Siponimod for Cognition in Secondary Progressive Multiple Sclerosis: Thinking Through the Evidence. *Neurology* 2021, 96(3):91-92.

25. Kulakowska A, Zendzian-Piotrowska M, Baranowski M, Kononczuk T, Drozdowski W, Gorski J, Bucki R: Intrathecal increase of sphingosine 1-phosphate at early stage multiple sclerosis. *Neurosci Lett* 2010, 477(3):149-152.

26. Qin J, Berdyshev E, Goya J, Natarajan V, Dawson G: Neurons and oligodendrocytes recycle sphingosine 1-phosphate to ceramide: significance for apoptosis and multiple sclerosis. *J Biol Chem* 2010, 285(19):14134-14143.

27. Kono M, Tucker AE, Tran J, Bergner JB, Turner EM, Proia RL: Sphingosine-1-phosphate receptor 1 in vivo. *J Clin Invest* 2014, 124(5):2076-2086.

28. Kono M, Proia RL: Imaging S1P1 activation in vivo. *Exp Cell Res* 2015, 333(2):178-182.

29. Guo SM, Yeh LH, Folkesson J, Ivanov IE, Krishnan AP, Keefe MG, Hashemi E, Shin D, Chhun BB, Cho NH *et al*: Revealing architectural order with quantitative label-free imaging and deep learning. *Elife* 2020, 9.

30. Tsai HC, Huang Y, Garris CS, Moreno MA, Griffin CW, Han MH: Effects of sphingosine-1-phosphate receptor 1 phosphorylation in response to FTY720 during neuroinflammation. *JCI Insight* 2016, 1(9):e86462.

31. Tsai HC, Nguyen K, Hashemi E, Engleman E, Hla T, Han MH: Myeloid sphingosine-1-phosphate receptor 1 is important for CNS autoimmunity and neuroinflammation. *J Autoimmun* 2019, 105:102290.

32. Arac A, Brownell SE, Rothbard JB, Chen C, Ko RM, Pereira MP, Albers GW, Steinman L, Steinberg GK: Systemic augmentation of alphaB-crystallin provides therapeutic benefit twelve hours post-stroke onset via immune modulation. *Proc Natl Acad Sci U S A* 2011, 108(32):13287-13292.

33. Benardais K, Kotsiari A, Skuljec J, Koutsoudaki PN, Gudi V, Singh V, Vulinovic F, Skripuletz T, Stangel M: Cuprizone [bis(cyclohexylidenehydrazide)] is selectively toxic for mature oligodendrocytes. *Neurotox Res* 2013, 24(2):244-250.

34. Miron VE, Jung CG, Kim HJ, Kennedy TE, Soliven B, Antel JP: FTY720 modulates human oligodendrocyte progenitor process extension and survival. *Ann Neurol* 2008, 63(1):61-71.

35. Coelho RP, Payne SG, Bittman R, Spiegel S, Sato-Bigbee C: The immunomodulator FTY720 has a direct cytoprotective effect in oligodendrocyte progenitors. *J Pharmacol Exp Ther* 2007, 323(2):626-635.

36. Jung CG, Kim HJ, Miron VE, Cook S, Kennedy TE, Foster CA, Antel JP, Soliven B: Functional consequences of S1P receptor modulation in rat oligodendroglial lineage cells. *Glia* 2007, 55(16):1656-1667.

37. Dukala DE, Soliven B: S1P1 deletion in oligodendroglial lineage cells: Effect on differentiation and myelination. *Glia* 2016, 64(4):570-582.

38. Zhang S, Zhu X, Gui X, Croteau C, Song L, Xu J, Wang A, Bannerman P, Guo F: Sox2 Is Essential for Oligodendroglial Proliferation and Differentiation during Postnatal Brain Myelination and CNS Remyelination. *J Neurosci* 2018, 38(7):1802-1820.

39. Zhu X, Bergles DE, Nishiyama A: NG2 cells generate both oligodendrocytes and gray matter astrocytes. *Development* 2008, 135(1):145-157.

40. Ozerdem U, Grako KA, Dahlin-Huppe K, Monosov E, Stallcup WB: NG2 proteoglycan is expressed exclusively by mural cells during vascular morphogenesis. *Dev Dyn* 2001, 222(2):218-227.

41. Polito A, Reynolds R: NG2-expressing cells as oligodendrocyte progenitors in the normal and demyelinated adult central nervous system. *J Anat* 2005, 207(6):707-716.

42. Rothhammer V, Kenison JE, Tjon E, Takenaka MC, de Lima KA, Borucki DM, Chao CC, Wilz A, Blain M, Healy L *et al*: Sphingosine 1-phosphate receptor modulation suppresses pathogenic astrocyte activation and chronic progressive CNS inflammation. *Proc Natl Acad Sci U S A* 2017, 114(8):2012-2017.

43. Mullershausen F, Craveiro LM, Shin Y, Cortes-Cros M, Bassilana F, Osinde M, Wishart WL, Guerini D, Thallmair M, Schwab ME *et al*: Phosphorylated FTY720 promotes astrocyte migration through sphingosine-1-phosphate receptors. *J Neurochem* 2007, 102(4):1151-1161.

44. Czech B, Pfeilschifter W, Mazaheri-Omrani N, Strobel MA, Kahles T, Neumann-Haefelin T, Rami A, Huwiler A, Pfeilschifter J: The immunomodulatory sphingosine 1-phosphate analog FTY720 reduces lesion size and improves neurological outcome in a mouse model of cerebral ischemia. *Biochem Biophys Res Commun* 2009, 389(2):251-256.

45. Gaire BP, Bae YJ, Choi JW: S1P1 Regulates M1/M2 Polarization toward Brain Injury after Transient Focal Cerebral Ischemia. *Biomol Ther (Seoul)* 2019:522-529.

46. Kim HJ, Miron VE, Dukala D, Proia RL, Ludwin SK, Traka M, Antel JP, Soliven B: Neurobiological effects of sphingosine 1-phosphate receptor modulation in the cuprizone model. *FASEB J* 2011, 25(5):1509-1518.

47. Kimura A, Ohmori T, Ohkawa R, Madoiwa S, Mimuro J, Murakami T, Kobayashi E, Hoshino Y, Yatomi Y, Sakata Y: Essential roles of sphingosine 1-phosphate/S1P1 receptor axis in the migration of neural stem cells toward a site of spinal cord injury. *Stem Cells* 2007, 25(1):115-124.

48. Yazdi A, Mokhtarzadeh Khanghahi A, Baharvand H, Javan M: Fingolimod Enhances Oligodendrocyte Differentiation of Transplanted Human Induced Pluripotent Stem Cell-Derived Neural Progenitors. *Iran J Pharm Res* 2018, 17(4):1444-1457.

49. Alfonso J, Penkert H, Duman C, Zuccotti A, Monyer H: Downregulation of Sphingosine 1-Phosphate Receptor 1 Promotes the Switch from Tangential to Radial Migration in the OB. *J Neurosci* 2015, 35(40):13659-13672.

50. Marques S, Zeisel A, Codeluppi S, van Bruggen D, Mendanha Falcao A, Xiao L, Li H, Haring M, Hochgerner H, Romanov RA *et al*: Oligodendrocyte heterogeneity in the mouse juvenile and adult central nervous system. *Science* 2016, 352(6291):1326-1329.

51. Yeung MS, Zdunek S, Bergmann O, Bernard S, Salehpour M, Alkass K, Perl S, Tisdale J, Possnert G, Brundin L *et al*: Dynamics of oligodendrocyte generation and myelination in the human brain. *Cell* 2014, 159(4):766-774.

52. Hasegawa Y, Suzuki H, Sozen T, Rolland W, Zhang JH: Activation of sphingosine 1-phosphate receptor-1 by FTY720 is neuroprotective after ischemic stroke in rats. *Stroke* 2010, 41(2):368-374.

53. Kajimoto T, Okada T, Yu H, Goparaju SK, Jahangeer S, Nakamura S: Involvement of sphingosine-1-phosphate in glutamate secretion in hippocampal neurons. *Mol Cell Biol* 2007, 27(9):3429-3440.

54. Groves A, Kihara Y, Jonnalagadda D, Rivera R, Kennedy G, Mayford M, Chun J: A Functionally Defined In Vivo Astrocyte Population Identified by c-Fos Activation in a Mouse Model of Multiple Sclerosis Modulated by S1P Signaling: Immediate-Early Astrocytes (ieAstrocytes). *eNeuro* 2018, 5(5).

55. Choi JW, Gardell SE, Herr DR, Rivera R, Lee CW, Noguchi K, Teo ST, Yung YC, Lu M, Kennedy G *et al*: FTY720 (fingolimod) efficacy in an animal model of multiple sclerosis requires astrocyte sphingosine 1-phosphate receptor 1 (S1P1) modulation. *Proc Natl Acad Sci U S A* 2011, 108(2):751-756.

56. Van Doorn R, Van Horssen J, Verzijl D, Witte M, Ronken E, Van Het Hof B, Lakeman K, Dijkstra CD, Van Der Valk P, Reijerkerk A *et al*: Sphingosine 1-phosphate receptor 1 and 3 are upregulated in multiple sclerosis lesions. *Glia* 2010, 58(12):1465-1476.

57. Zamanian JL, Xu L, Foo LC, Nouri N, Zhou L, Giffard RG, Barres BA: Genomic analysis of reactive astrogliosis. *J Neurosci* 2012, 32(18):6391-6410.

58. Rivera J, Proia RL, Olivera A: The alliance of sphingosine-1-phosphate and its receptors in immunity. *Nat Rev Immunol* 2008, 8(10):753-763.

59. Allende ML, Tuymetova G, Lee BG, Bonifacino E, Wu YP, Proia RL: S1P1 receptor directs the release of immature B cells from bone marrow into blood. *J Exp Med* 2010, 207(5):1113-1124.

60. Liu G, Burns S, Huang G, Boyd K, Proia RL, Flavell RA, Chi H: The receptor S1P1 overrides regulatory T cell-mediated immune suppression through Akt-mTOR. *Nat Immunol* 2009, 10(7):769-777.

61. Maeda Y, Seki N, Kataoka H, Takemoto K, Utsumi H, Fukunari A, Sugahara K, Chiba K: IL-17-Producing Vgamma4+ gammadelta T Cells Require Sphingosine 1-Phosphate Receptor 1 for Their Egress from the Lymph Nodes under Homeostatic and Inflammatory Conditions. *J Immunol* 2015, 195(4):1408-1416.

62. Muller J, von Bernstorff W, Heidecke CD, Schulze T: Differential S1P Receptor Profiles on M1- and M2-Polarized Macrophages Affect Macrophage Cytokine Production and Migration. *Biomed Res Int* 2017, 2017:7584621.

63. Challen GA, Goodell MA: Promiscuous expression of H2B-GFP transgene in hematopoietic stem cells. *PLoS One* 2008, 3(6):e2357.

64. Morcos MNF, Zerjatke T, Glauche I, Munz CM, Ge Y, Petzold A, Reinhardt S, Dahl A, Anstee NS, of primitive hematopoietic stem cells in adult mice. *J Exp*

Med 2020, 217(6).

65. Cartier A, Leigh T, Liu CH, Hla T: Endothelial sphingosine 1-phosphate receptors promote vascular normalization and antitumor therapy. *Proc Natl Acad Sci U S A* 2020, 117(6):3157-3166.

66. Ebenezer DL, Fu P, Suryadevara V, Zhao Y, Natarajan V: Epigenetic regulation of pro-inflammatory cytokine secretion by sphingosine 1-phosphate (S1P) in acute lung injury: Role of S1P lyase. *Adv Biol Regul* 2017, 63:156-166.

67. Fu P, Ebenezer DL, Ha AW, Suryadevara V, Harijith A, Natarajan V: Nuclear lipid mediators: Role of nuclear sphingolipids and sphingosine-1-phosphate signaling in epigenetic regulation of inflammation and gene expression. *J Cell Biochem* 2018, 119(8):6337-6353.

68. Jean-Charles PY, Kaur S, Shenoy SK: G Protein-Coupled Receptor Signaling Through beta-Arrestin-Dependent Mechanisms. *J Cardiovasc Pharmacol* 2017, 70(3):142-158.

69. Pyne NJ, Pyne S: Sphingosine 1-Phosphate Receptor 1 Signaling in Mammalian Cells. *Molecules* 2017, 22(3).

Figures

Fig.1

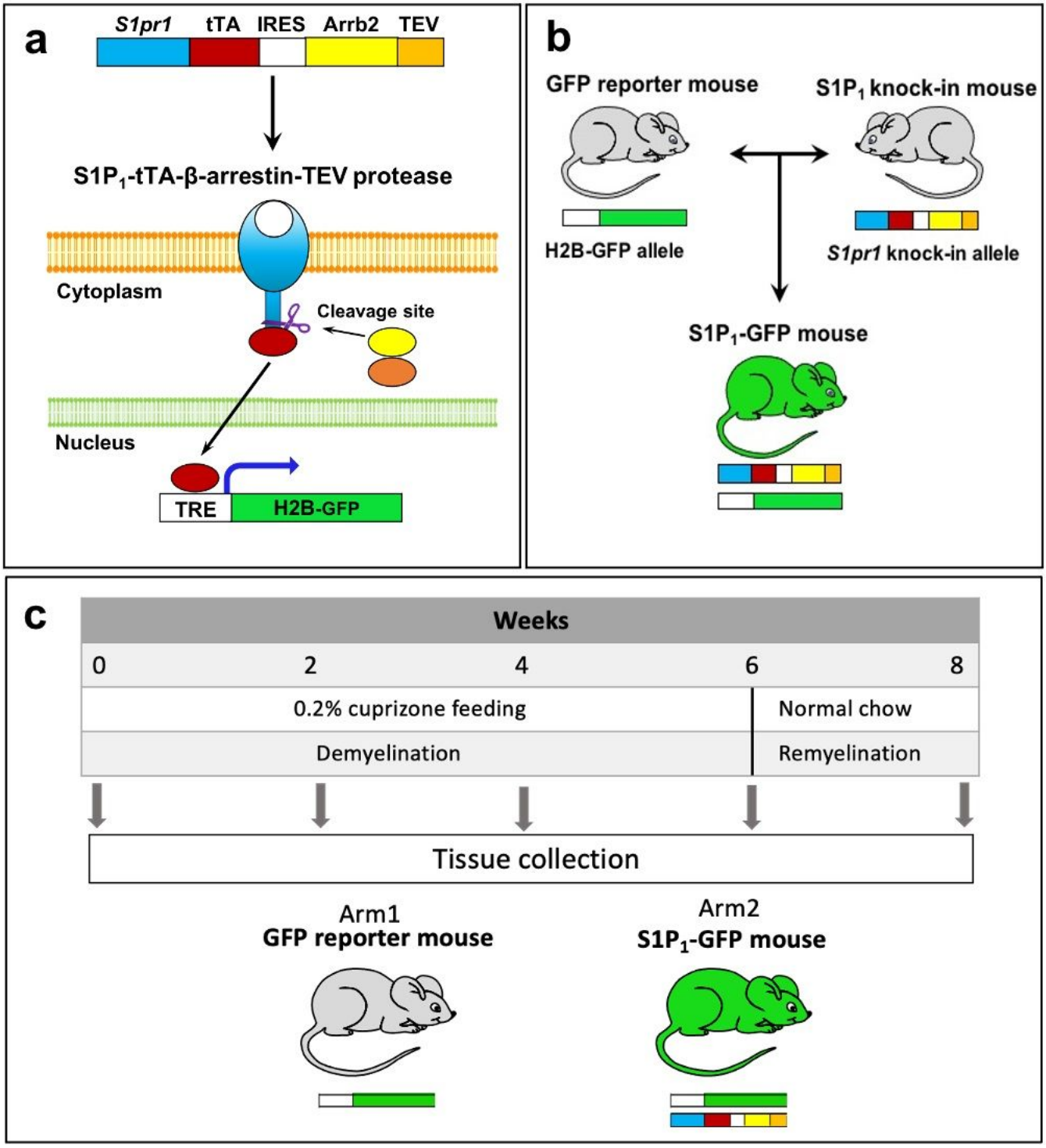

Figure 1

Generation of S1P1-GFP signaling mice using the Tango system. (a) Diagram depicting generation of the S1pr1 knock-in allele. The S1pr1 knock-in vector is constructed using two sets of fusion genes, TEV protease cleavage site and tTA linked to S1P1 C terminal, and β-arrestin-2 linked to TEV protease (Arrb2-TEV). The two fusion genes connected via an IRES segment. S1P-S1P1 interaction results in the coupling

protein and initiates the release of tTA from the C terminus of

modified S1P1. Free tTA transfers to the nucleus and initiates GFP expression in histone-EGFP reporter (H2B-GFP) mice. Diagram adapted from Kono et al (2014). (b) S1P1 knock-in mice are crossed with H2B-GFP mice to generate S1P1-GFP signaling mice. (c) Experimental design of the cuprizone-induced demyelination model. Arrb2; β-arrestin-2, TEV; Tobacco etch virus, tTA; tetracycline-controlled transactivator, IRES; internal ribosome entry site, GFP; Green fluorescence protein, S1pr1; S1P receptor 1 gene, S1P1; S1P receptor 1.

Fig. 2

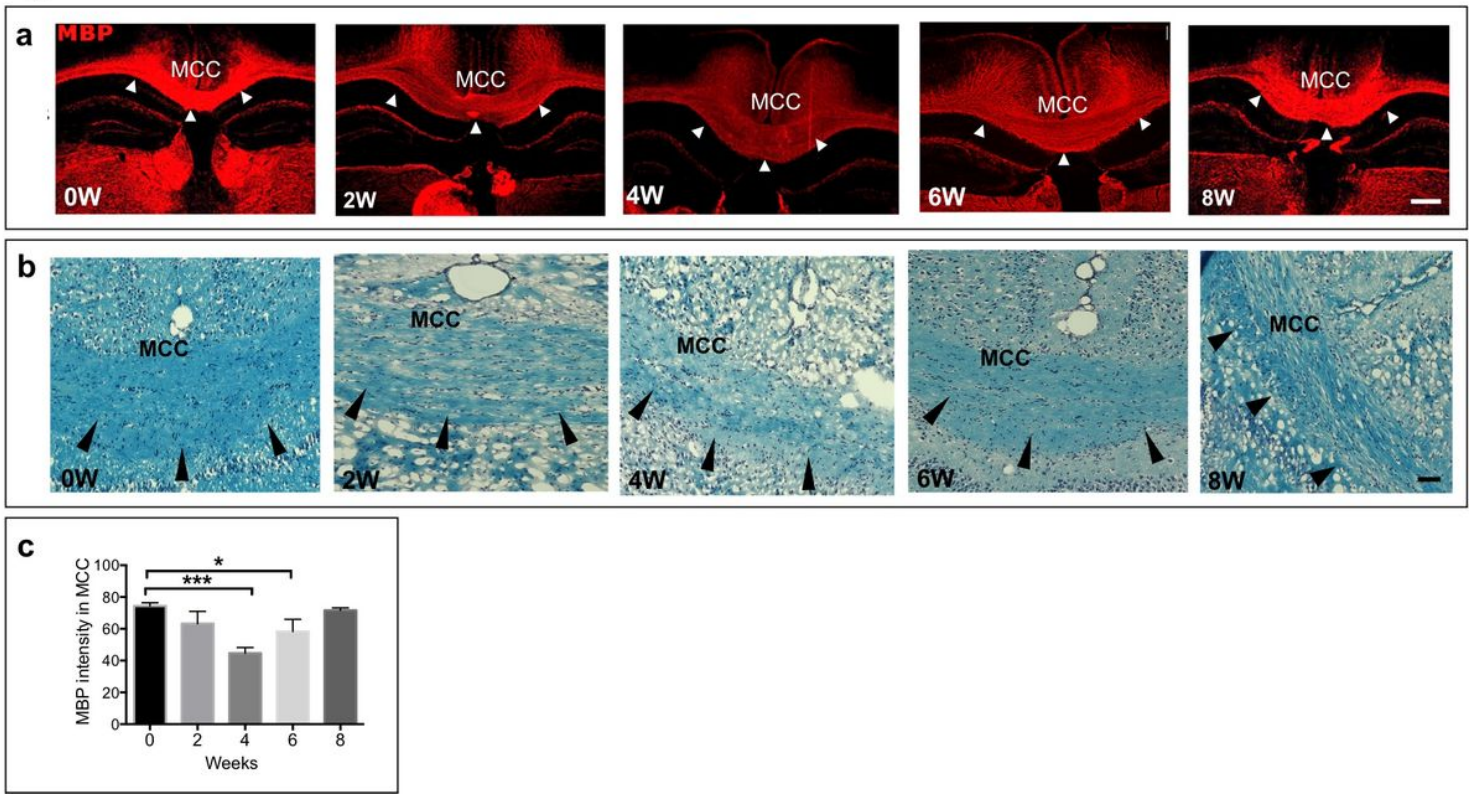

Figure 2

Validation of cuprizone-induced demyelination in S1P1-GFP signaling mice. (a) Immunohistochemistry using MBP staining of the brain depicting de/remyelination in the MCC (arrowhead) of S1P1-GFP signaling mice following exposure to cuprizone diet (0-8 weeks). Scale bar, 200 μm. (b) LFB staining depicting myelination in the MCC (arrowhead) of S1P1-GFP mice upon cuprizone exposure (0-8 weeks), Scale bar, 50 μm. (c) Quantification of MBP intensity in the MCC of S1P1-GFP signaling mice fed with cuprizone diet from (a), (n=3 mice /group). Values shown are expressed as mean ± SEM. Statistical significance was determined by unpaired t-test, *p<0.05, ***p<0.001. MCC; Medial corpus callosum, LFB; Luxol Fast Blue, MBP; myelin basic protein.

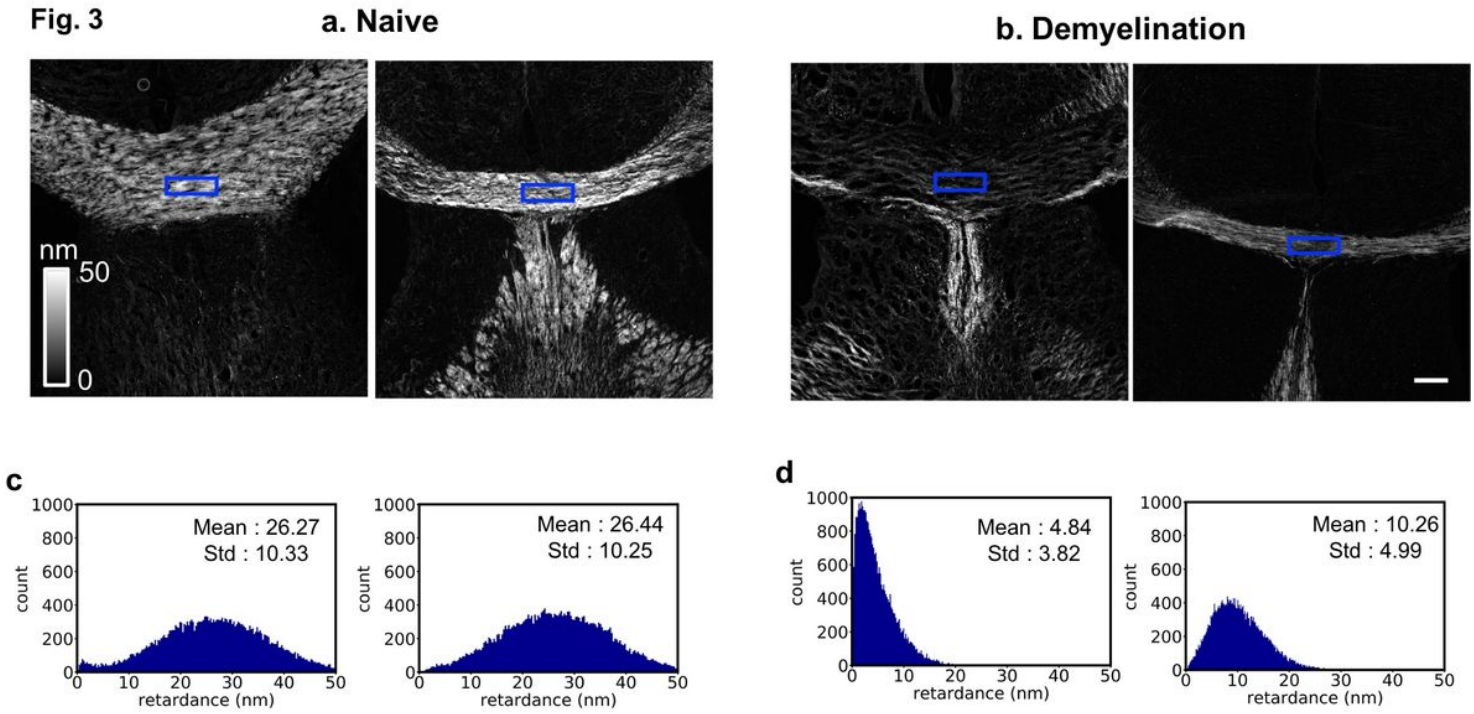

Figure 3

Validation of cuprizone-induced demyelination by quantitative label-free microscopy. Retardance intensity from myelin anisotropy in the MCC of (a) naïve and (b) cuprizone diet-fed (4 weeks) S1P1-GFP signaling mice (n=2/group). The grayscale color bar indicates the range of displayed retardance measurement in the unit of nanometer (nm). The histograms of the signals from the blue-box areas in the MCC of brain sections show retardance of myelin (nm) from naïve mice from (a) (c), and cuprizone diet-fed mice (from b) (d). The Y axis of histogram represent the number of pixels in the bin with ~ 0.3 nm. Scale bar, 200 μm. MCC; Medial corpus callosum.

Fig. 4

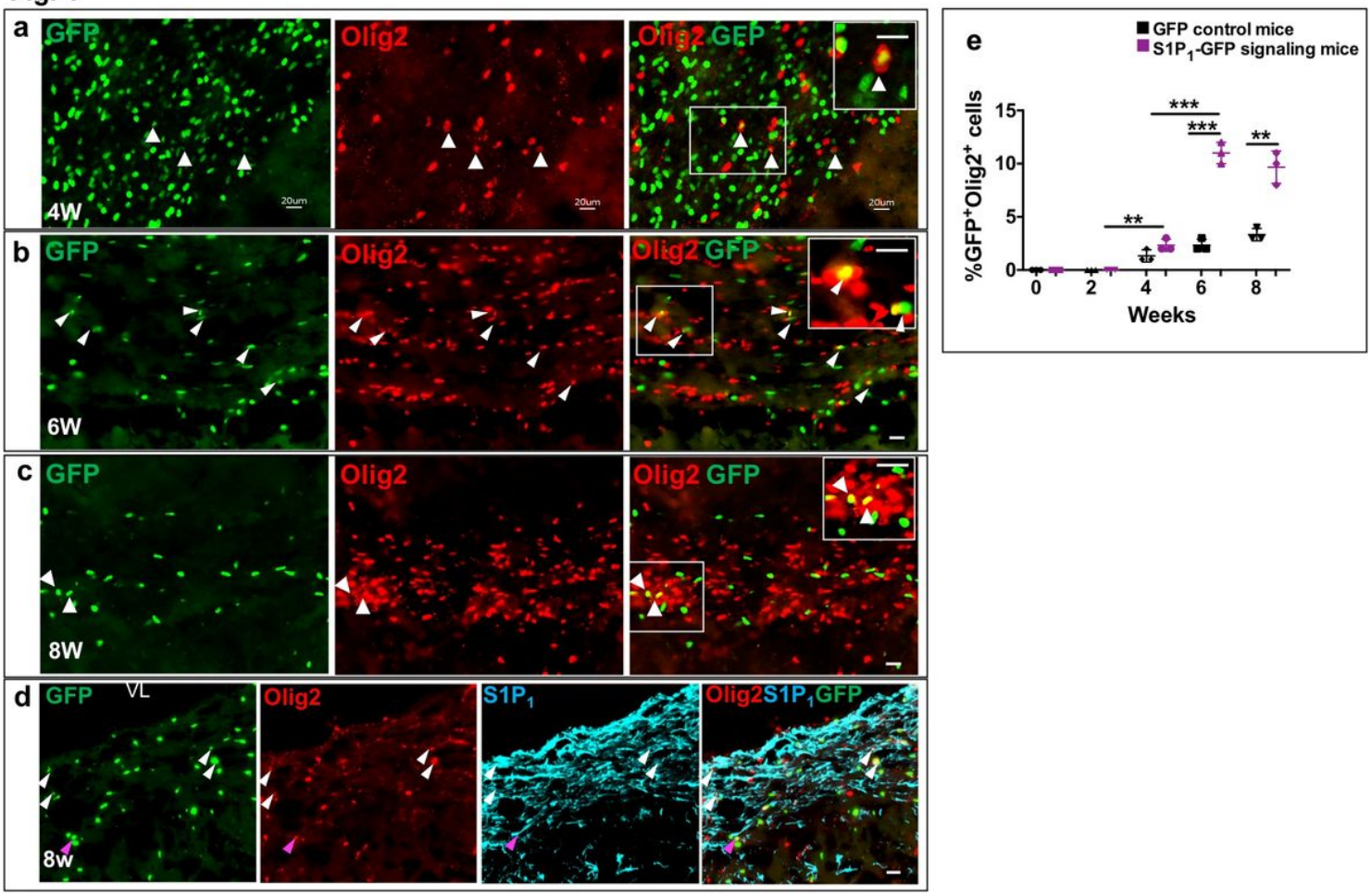

Figure 4

S1P1 signaling in oligodendrocytes depicted by GFP expression during remyelination. (a) Immunohistochemistry of oligodendrocytes (Olig2+) in the MCC of S1P1-GFP signaling mice at 4 weeks, (b) 6 weeks and (c) 8 weeks following exposure to cuprizone diet. White arrowheads indicate GFP expression colocalizing with Olig2+. Magnification of S1P1 signaling in oligodendrocytes is depicted in the upper right corner. (d) S1P1 and Olig2 staining in the SVZ of S1P1-GFP signaling mice at 8 weeks of cuprizone diet. White arrowheads represent GFP expression in Olig2+S1P1+ cells and magenta arrowheads represent GFP expression in Olig2+S1P1- cells. The image on the right shows a higher magnification of GFP expression in Olig2+NG2+ cells. Scale bars, 20 μm. (e) Quantification of GFP+Olig2+ to the total GFP+ cells in 0.1 mm2 of MCC of the control and S1P1-GFP signaling mice, (n=3 mice/group). ImageJ used for counting the cells, values shown are expressed as mean ± SEM. Unpaired t-test was used to compare significant difference between the two groups, **p<0.01, ***p<0.001. SVZ; subventricular zone. MCC; Medial corpus callosum, OPCs; Oligodendrocyte progenitor cells and NG2; Neural/glial antigen.

Fig. 5

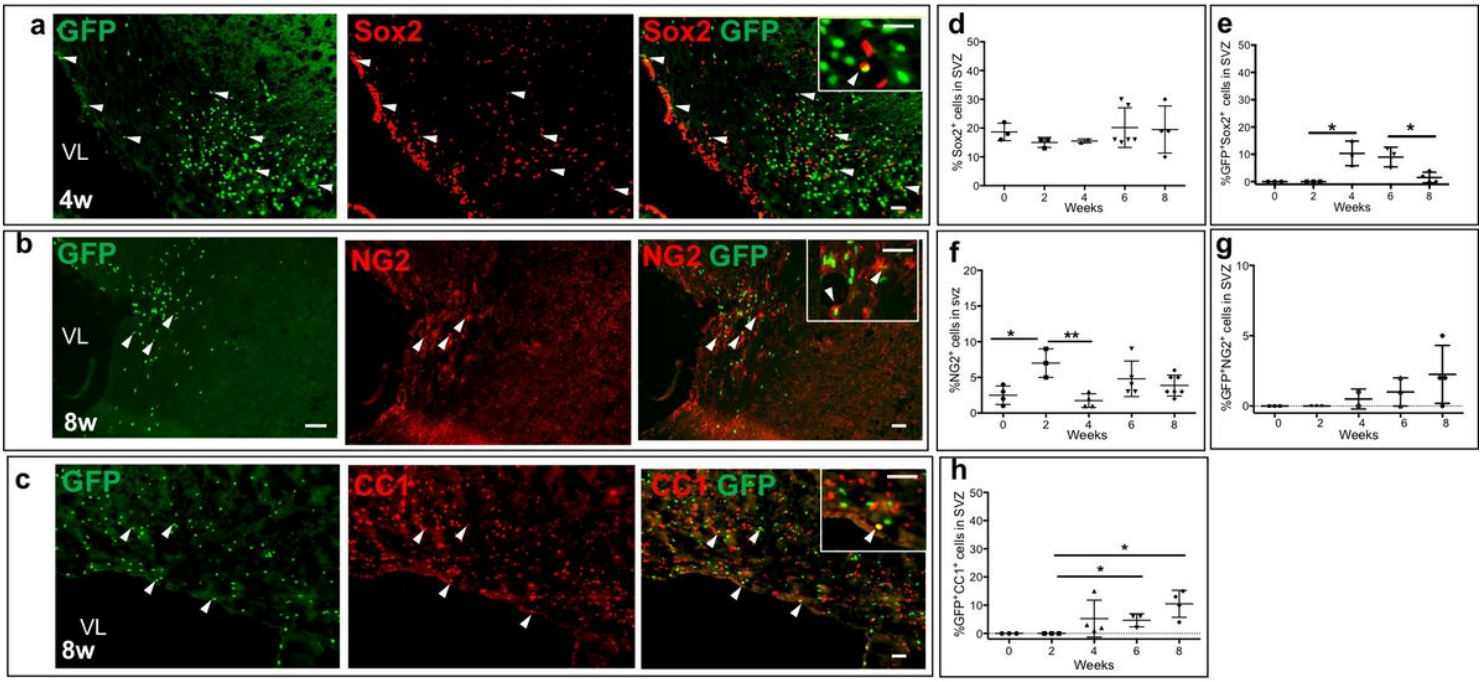

Figure 5

S1P1 signaling in oligodendrocyte progenitor cells detected by GFP expression. The images represent S1P1 signaling in (a) Sox2+ (b) NG2+ and (c) CC1+ cells in SVZ of S1P1-GFP signaling mice at 4 (a) and 8 (b and c) weeks following exposure to cuprizone. Arrowheads indicate colocalization with GFP signal. The upper right corner images depict higher magnification of S1P1 signaling in oligodendrocyte progenitor cells. The graphs represent the percentage of (d) Sox2+ and (f) NG2+ cells in 0.1 mm2 SVZ of S1P1-GFP signaling mice and normalized by DAPI, n=3-6 mice/groups. The percentage of (e) GFP+Sox2+, (g) GFP+NG2+ and (h) GFP+CC1+ cells of total GFP+ cells per 0.1 mm2 of SVZ during cuprizone diet (0, 2, 4, 6, and 8 weeks), n=3-6 mice/groups. Values shown are expressed as mean ± SEM. Unpaired t-test was used to compare significant difference between the two groups, *p<0.05, **p<0.01. SVZ; subventricular zone. Scale bars: 20 µm. SVZ; Subventricular zone. NG2; Neural/glial antigen 2., VL; Lateral ventricle.

Fig. 6

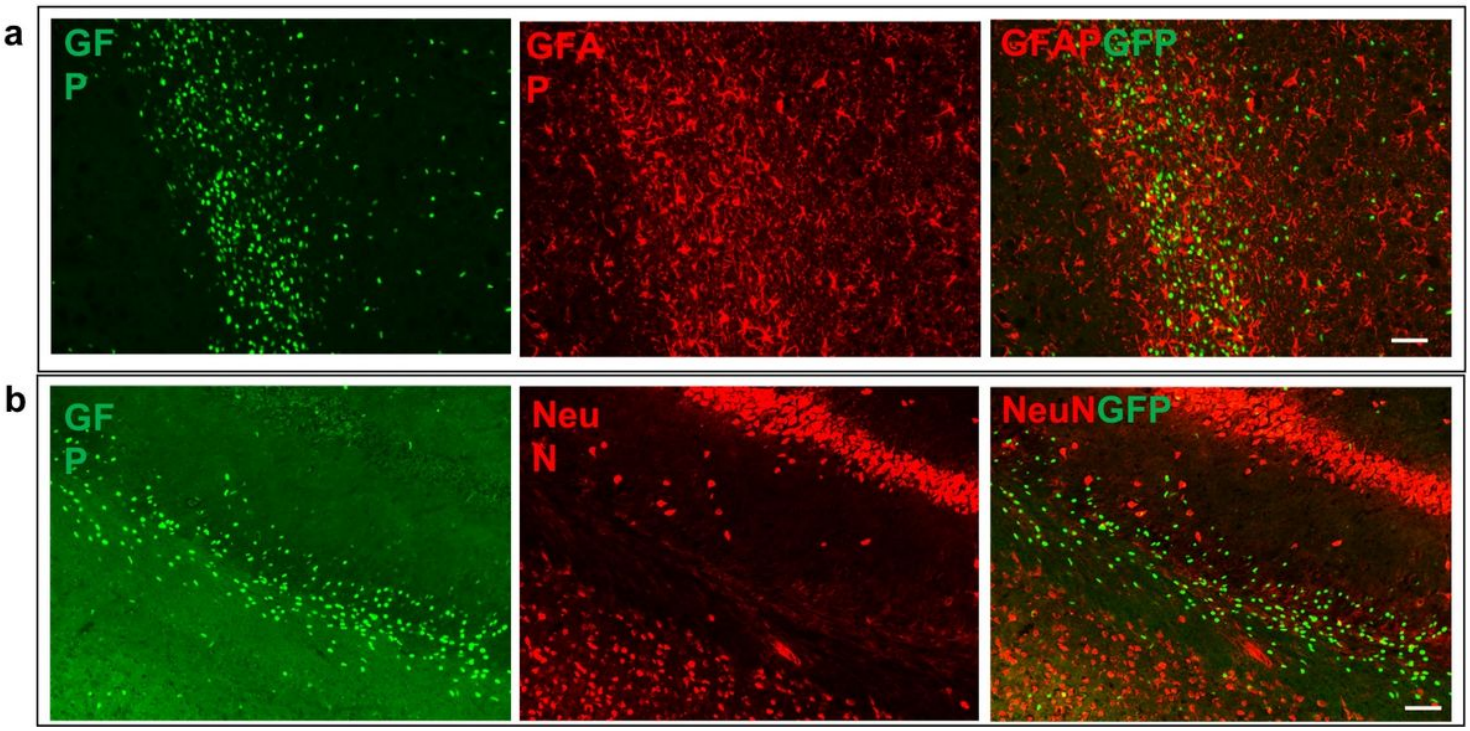

Figure 6

Lack of GFP expression in astrocytes and neurons in S1P1-GFP signaling mice during cuprizone diet. The images indicated (a) Astrocytes (GFAP+) and (b) NeuN+ cells were GFP negative in the LCC of S1P1-GFP signaling mice at 4 weeks of cuprizone diet. scale bars, 50 μm (a and b). LCC; Lateral corpus callosum.

Fig. 7

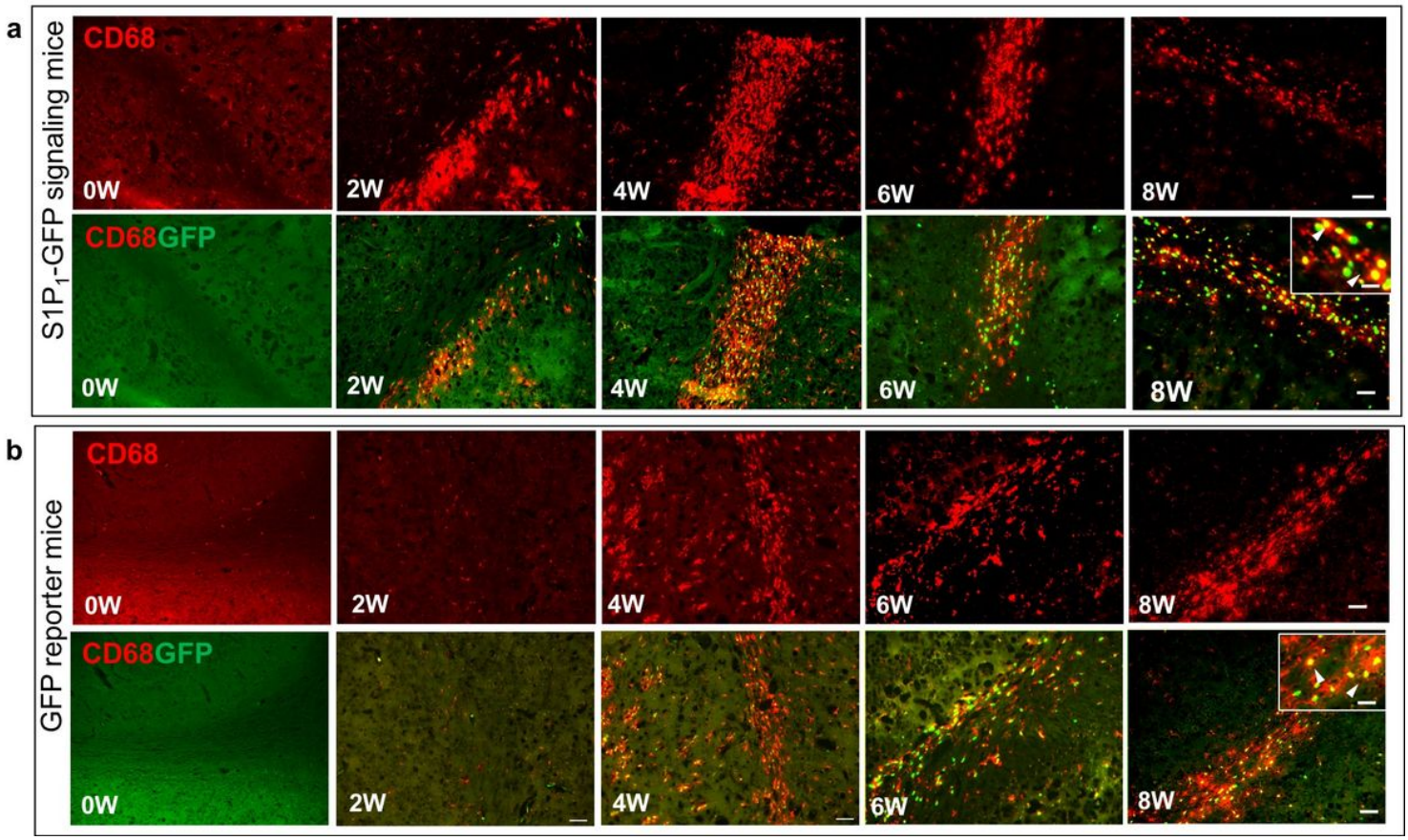

Figure 7

GFP expression in myeloid cells of S1P1-GFP signaling and GFP reporter mice upon cuprizone exposure. GFP expression in myeloid cells (CD68+) in the LCC of (a) S1P1-GFP signaling mice and (b) GFP reporter mice at 0, 2, 4, 6, 8 weeks of the cuprizone diet. In the upper right corner higher magnification of GFP expression in CD68+ cells are shown. Scale bars; 50 μm and 20 μm for images with higher magnification. LCC; Lateral corpus callosum.

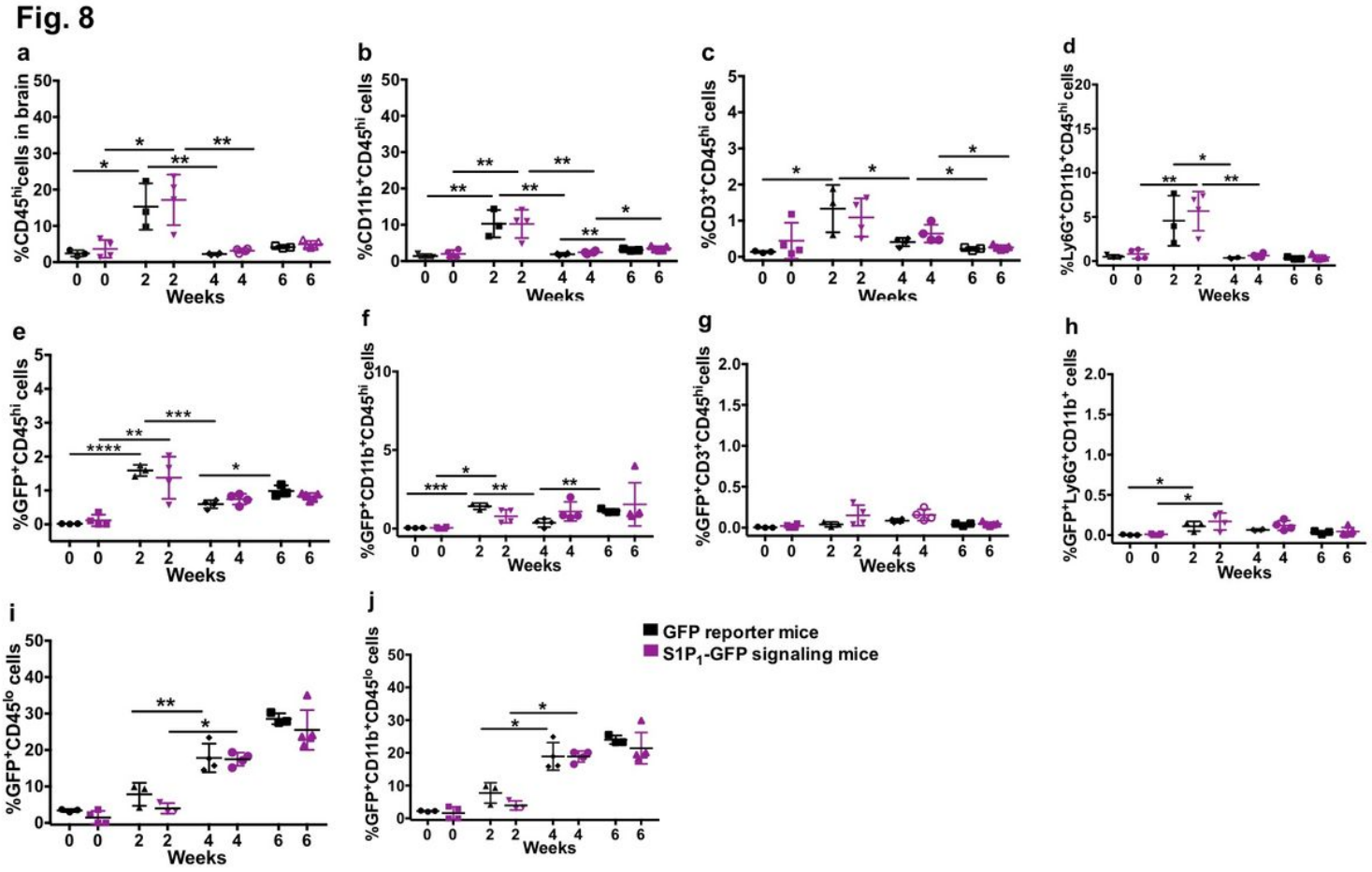

Figure 8

Flow cytometry analysis of S1P1 signaling via GFP expression in cerebral immune cells upon cuprizone-induced demyelination. GFP expression in cerebral immune cell subpopulations upon cuprizone exposure (0, 2, 4 and 6 weeks) in GFP reporter and S1P1-GFP signaling mice. (a) Infiltration of immune cells (CD45hi), (b) myeloid cells (CD11b+CD45hi), (c) lymphocytes (CD3+CD45hi) and (d) granulocytes (LyG+CD45hi) into the brain during demyelination (0-6 weeks) in S1P1-GFP signaling and GFP reporter mice. (e) GFP expression in infiltrating immune cells (CD45hi), (f) myeloid cells (CD11b+CD45hi), (g) lymphocytes (CD3+CD45hi) and (h) granulocytes (LyG+CD45hi) in GFP reporter and S1P1-GFP signaling mice during demyelination. GFP expression in (i) resident microglia GFP+CD45lo and (j) GFP+CD45lo CD11b+ in GFP reporter and signaling mice. Values shown are expressed as mean ± SEM. Unpair t-test was used to analyze significant difference between two groups. *p<0.05, **p<0.01, ***P<0.001, and ****P<0.0001.

Fig. 9

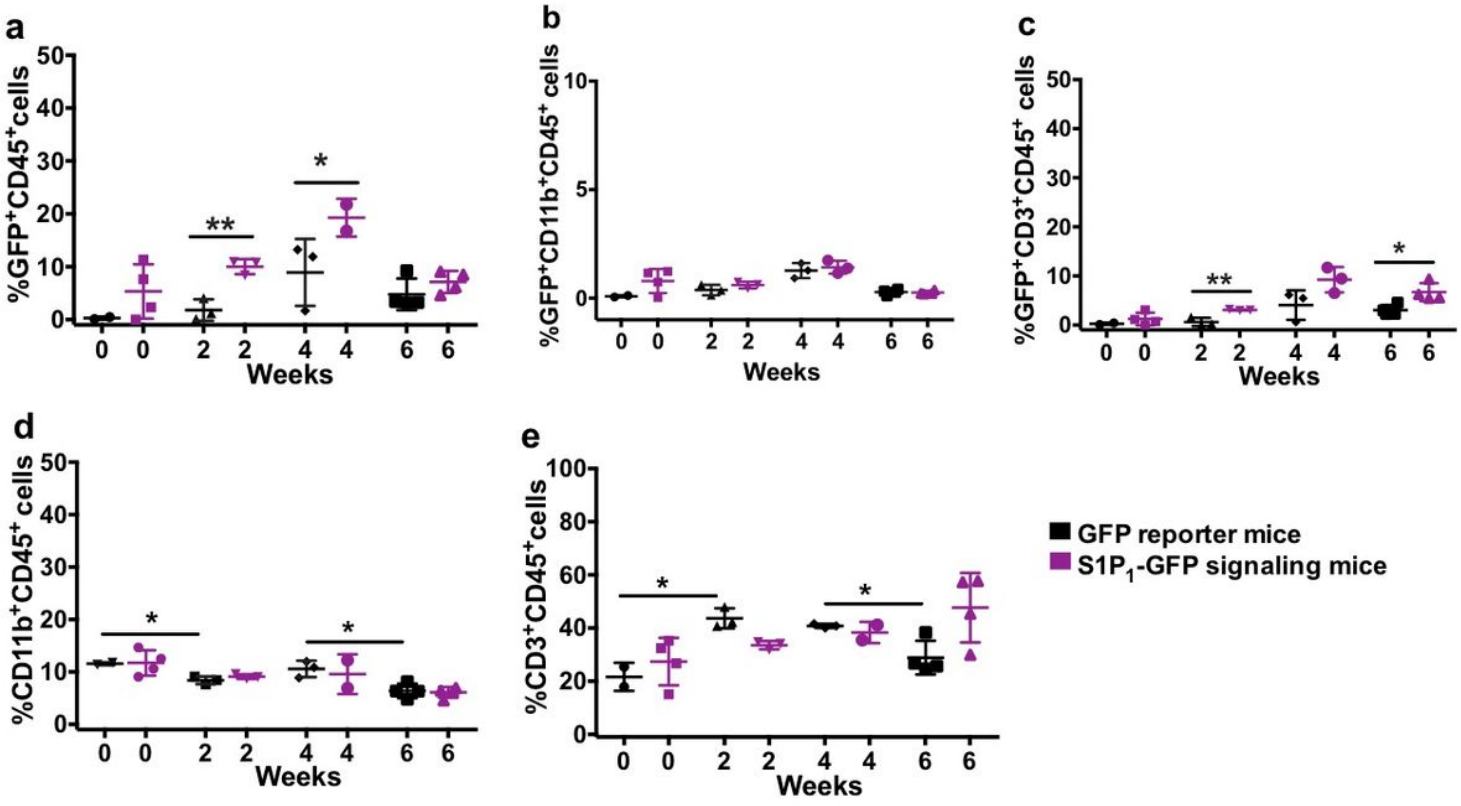

Figure 9

Flow cytometry analysis of S1P1 signaling via GFP expression in splenic immune cells upon cuprizone-induced demyelination. (a) GFP expression in leukocytes (CD45+), (b) myeloid cells (CD11b+) and (c) lymphocytes (CD3+) in the spleens of S1P1-GFP signaling and GFP reporter mice following exposure to cuprizone diet (0-6 weeks). (d) Percentage of myeloid cells (CD11b+) and l (e) lymphocytes in CD45+ population during cuprizone diet. Values shown are expressed as mean ± SEM. Unpair t-test was used to analyze significant difference between two groups, *p<0.05 and **p<0.01.

Supplementary Files

This is a list of supplementary files associated with this preprint. Click to download.

- Fig6S.tif
- Fig1S.tif
- Fig2S.tif
- Fig3S.tif
- Fig4S.tif
- Fig5S.tif

- Fig7S.tif
- Fig8S.tif
- Fig9S.tif
- suplementarylegends.docx